https://doi.org/10.5194/egusphere-2026-2557
Preprint. Discussion started: 15 June 2026

Decoupling between local precipitation and deep groundwater recharge in a tropical sedimentary basin: Evidence from stable isotopes

Luciana Maria Ferrer[1], Laura De Simone Borma[2], Carlos Daniel Meneghetti[2], Breno Pupin[2], Fábio Hitoshi Sakaguchi[2], Rita de Cassya Almeida Sousa[2]

[1]Engineering, Modeling and Applied Social Sciences Center, Federal University of ABC (UFABC), Santo André, 09210-580, Brazil

[2]Isotopic Ecohydrology Laboratory, Impacts, Adaptation, and Vulnerabilities Division, General Coordination of Earth Sciences, National Institute for Space Research (INPE), São José dos Campos, 12227-010, Brazil

Correspondence to: Luciana Maria Ferrer (luciana.ferrer@ufabc.edu.br)

Abstract. Groundwater recharge in sedimentary basins is often assumed to be locally controlled, yet increasing evidence suggests the importance of spatially distributed and multi-scale processes. Here, we investigate the controls on groundwater recharge in the Taubaté Sedimentary Basin (southeastern Brazil) using stable isotopes ($\delta^{18}O$ and $\delta^{2}H$), d-excess, and electrical conductivity data from precipitation, springs, and deep wells. Results reveal a clear decoupling between local precipitation and deep groundwater recharge. Most groundwater samples plot below the Local Meteoric Water Line (LMWL) and exhibit reduced regression slopes, indicating the influence of mixing, delayed percolation, and non-conservative recharge processes. Deep groundwater shows low isotopic variability and weak seasonal signals, consistent with longer residence times and regional flow integration. In contrast, spring waters display greater variability and stronger sensitivity to seasonal inputs and near-surface processes. A closer isotopic correspondence between deep groundwater and precipitation from higher-altitude areas suggests that effective recharge occurs preferentially in elevated zones and is subsequently redistributed toward lower basin sectors. Electrical conductivity and d-excess relationships further indicate that shallow groundwater is influenced by evaporation and short flow paths. Together, these findings support a conceptual model of a dual groundwater system, characterized by the coexistence of rapid, shallow flow paths and slower, regionally integrated deep circulation. This study highlights the importance of spatially decoupled recharge and cross-scale groundwater dynamics for understanding hydrological functioning in sedimentary basins.

1 Introduction

The intensification of global water consumption, combined with the increasing frequency of extreme weather events, has placed water supplies for human population at growing risk. Global warming, by altering precipitation regimes and evapotranspiration patterns, compromises surface water availability and increases reliance on groundwater resources, which represent a strategic alternative for water supply (Vörösmarty et al., 2000). However, the extensive and often unregulated exploitation of these resources has led to aquifer depletion, rendering them effectively non-renewable in several regions of the world (Döll et al., 2014). In this context, understanding the hydrological processes that control aquifer recharge, together with the implementation of sustainable management practices, is essential to mitigate the impacts of current and future water crises, as well as to support ecosystem conservation and restoration. At the local scale, assessing the spatial and seasonal variability of recharge is fundamental for water supply planning, sanitation management, and the mitigation of water-related risks (Oliveira & Salati, 1981; Bedaso & Wu, 2021).

Isotopic analysis of natural waters, based on $\delta^{18}O$ and $\delta^{2}H$ ratios, has become a fundamental tool for identifying water sources,

https://doi.org/10.5194/egusphere-2026-2557
Preprint. Discussion started: 15 June 2026

flow paths, and the hydrological processes that regulate the dynamics of aquatic systems (Clark & Fritz, 1997; Barbosa et al., 2018; Yoshioka & Yoshioka, 2022). The isotopic composition of water is sensitive to processes such as evaporation and condensation, undergoing characteristic fractionation throughout the hydrological cycle that provides a distinctive geochemical fingerprint (Epstein & Mayeda, 1953; Friedman, 1953; Craig, 1961; Cherry et al., 2020). Advances in analytical techniques, particularly laser spectroscopy, have enabled rapid, precise, and relatively low-cost measurements of these isotopes (Gupta et al., 2009), significantly expanding the application of isotopic approaches in studies of aquifer recharge and water balance across a wide range of climatic regions (Jasechko et al., 2014).

In addition to climatic factors, changes in land use and land cover significantly influence recharge dynamics. Water salinity, resulting from both natural processes and anthropogenic activities, serves as an indicator of groundwater quality and the degree of human interference in aquifer systems (Jobbágy and Jackson, 2004; Estévez et al., 2018). Electrical conductivity (EC), as a proxy for dissolved ion content, is widely used to detect contamination and to distinguish hydrogeological processes occurring in recharge and discharge zones. The integrated analysis of EC and deuterium excess (d-excess) has been applied to evaluate interactions between surface water and groundwater (Tirumalesh et al., 2017; Liberoff and Poca, 2023), enabling inferences about processes such as evapotranspiration, preferential recharge, and vertical water exchanges within the unsaturated zone.

In Brazil, the Taubaté Sedimentary Basin constitutes an important aquifer system in the Southeast region, where groundwater exploitation has intensified in recent decades. The study area, located in the municipality of São José dos Campos, in the Paraíba Valley, lies between the two largest metropolitan centers in the country—São Paulo and Rio de Janeiro. The municipality provides water supply and sewage infrastructure to 99.6% of its urban population, serving more than 750,000 inhabitants, and hosts a major industrial complex. Of the 2,218 wells registered in the Paraíba do Sul River hydrographic domain, 406 are located in São José dos Campos (SGB, 2023). Rapid urban expansion, with an annual population growth rate of 0.95% (IBGE, 2023), has intensified pressure on water resources and increased the vulnerability of urban infrastructure to climate variability and change (IPCC, 2022).

Despite the growing dependence on groundwater resources in the region, there is still limited understanding of the relative contribution of seasonal precipitation to aquifer recharge and of the connectivity between shallow and deep groundwater systems. Addressing these knowledge gaps is essential for improving water resource management strategies and enhancing resilience to climate variability.

In this context, this study aims to: (i) apply stable isotope techniques (δ^2H and $\delta^{18}O$) to evaluate the isotopic similarity between groundwater from springs and deep wells within the Taubaté Sedimentary Basin and the adjacent alluvial aquifer system; and (ii) assess the contribution of seasonal precipitation to aquifer recharge dynamics.

2. Materials and Methods

2.1 Study area

The study was conducted in the municipality of São José dos Campos (SP), located in the central eastern portion of the state of São Paulo, between the Serra do Mar and Serra da Mantiqueira mountain ranges. With a total area of 1,099.6 km², the municipality lies within the São Paulo section of the Paraíba do Sul River basin, one of the main water management units in

https://doi.org/10.5194/egusphere-2026-2557
Preprint. Discussion started: 15 June 2026

southeastern Brazil (Figure 1).

The regional climate is humid tropical with dry winter and hot summer (Cwa), according to the Köppen-Geiger classification. It is characterized by hot, rainy summers and mild, dry winters. The mean annual temperature is 20.3 °C, and the mean annual precipitation ranges from 1,300 and 1,400 mm (Gama et al., 2003; Climate Data, 2023; INMET, 2023). The hydrological year extends from October to September, with the rainy season occurring between October and March and the dry season between April and September (ANA, 2023; CEMADEN, 2023; INMET, 2023).

From a geological and hydrogeological perspective, São José dos Campos is situated within the Taubaté Sedimentary Basin, one of the main structural units of the Southeastern Brazilian Continental Rift, formed by extensional tectonic processes initiated during the Eocene (Riccomini, 1989; Vidal et al. 2004; SBG, 2023). The sedimentary fill of the basin comprises Paleogene and Neogene chronostratigraphic units, including the Resende, Tremembé, and São Paulo Formations (Paleogene) and the Pindamonhangaba Formation (Neogene), in addition to Quaternary alluvial deposits (Fig. 1).

The Resende Formation (Paleocene–Eocene) consists predominantly of fine- to medium-grained sandstones interbedded with claystones and siltstones, deposited in braided fluvial systems and alluvial fans. This unit hosts semi-confined aquifers of moderate productivity, characterized by relatively high permeability in sandy facies and pronounced lateral heterogeneity. The Tremembé Formation (Oligocene) is composed mainly of shales, marls, and micritic limestones rich in organic matter and fossils, deposited in lacustrine and palustrine environments. Due to the marked intercalation of compact, low-permeability claystones with more permeable sandy layers, this unit acts predominantly as an aquitard, restricting vertical groundwater flow and creating a hydraulic discontinuity between the aquifers of the Resende and São Paulo formations.

The São Paulo Formation (Oligocene–Miocene) comprises sandstones, sandy–clayey conglomerates, and interbedded clay and silt layers deposited in meandering fluvial systems and floodplain environments. Although its regional extent within the Taubaté Basin is limited, it represents one of the main outcropping units in the study area and is widely exploited by deep tubular wells in the municipality. Its hydraulic conductivity is variable, reflecting differences in sediment texture, cementation, and the proportion of sandy fractions.

The overlying Pindamonhangaba Formation (Miocene–Pliocene) consists of arkosic sandstones and poorly sorted conglomerates with a clay-rich matrix. These deposits correspond to the final stage of basin infill and display low lateral continuity, forming local and discontinuous aquifers of limited extent.

At the surface, Quaternary alluvial deposits, composed of poorly consolidated sands, gravels, and silts, dominate the floodplains of the Paraíba do Sul River and its tributaries. These materials form highly permeable unconfined aquifers, directly recharged by precipitation and surface runoff, and constitute the principal recharge zones of the local hydrogeological system.

The superposition of sedimentary units of different ages and depositional environments results in pronounced hydrogeological heterogeneity, characterized by vertical and lateral contrasts in permeability and distinct groundwater residence times. This complex structural framework controls both direct and indirect recharge mechanisms and influences the isotopic signatures observed in spring waters and deep wells analyzed in this study.

https://doi.org/10.5194/egusphere-2026-2557
Preprint. Discussion started: 15 June 2026

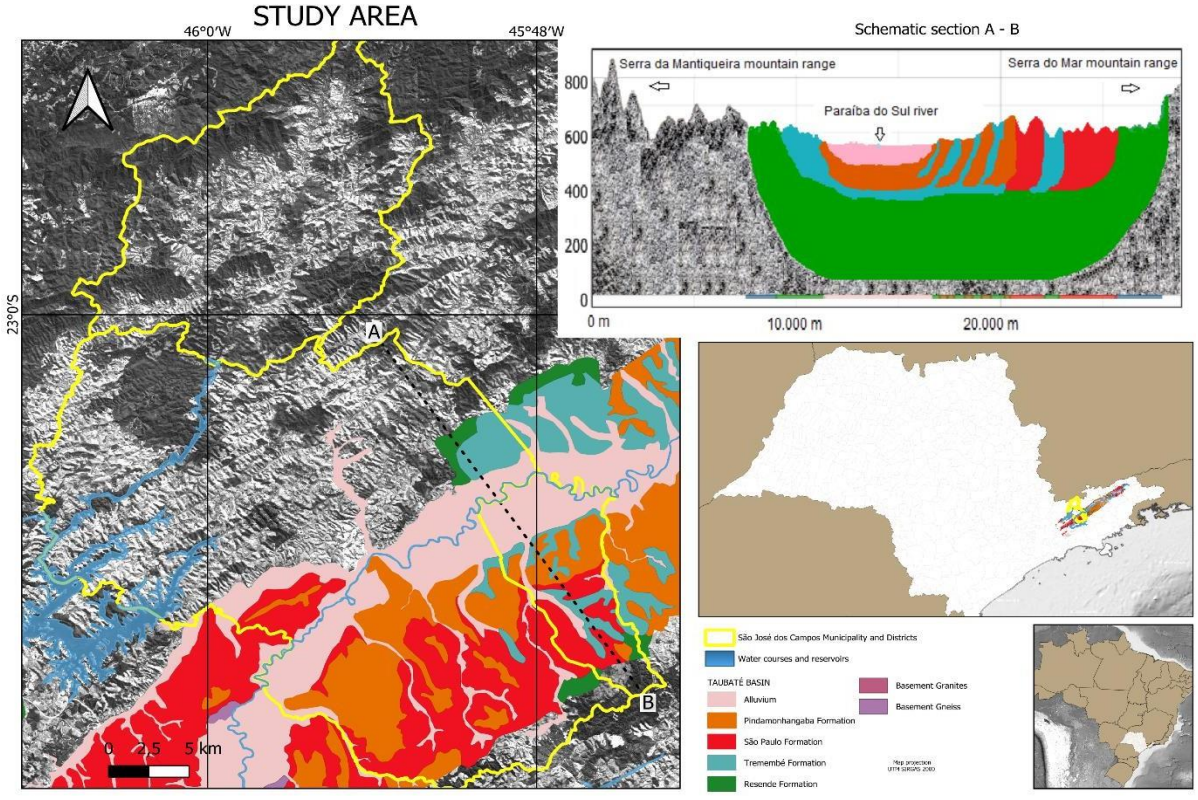

Figure 1. Location and geological setting of the study area. Groundwater abstraction is concentrated in the most densely populated area of the municipality of São José dos Campos, located within the Paraíba do Sul River basin and the Taubaté Sedimentary Basin. The schematic cross-section highlights the main geological units of the region. (Source: the authors).

2.2 Groundwater sampling

Groundwater samples were collected from deep tubular wells and springs distributed across the southern, eastern, western, and southeastern sectors of municipality (Fig. 2a and 2b).

For deep well sampling, 20 tubular wells authorized by SP Águas (2025) were selected to represent the main aquifer systems in the study area. Spring sampling points were defined based on the inventory provided by the Municipal Government of São José dos Campos (Sundfeld et al., 2021), totaling 24 springs distributed across areas with different vegetation cover and topographic conditions (Appendix material). Deep wells are identified as W (e.g., W50), while spring sampling sites are labeled as S (e.g., S7).

https://doi.org/10.5194/egusphere-2026-2557
Preprint. Discussion started: 15 June 2026

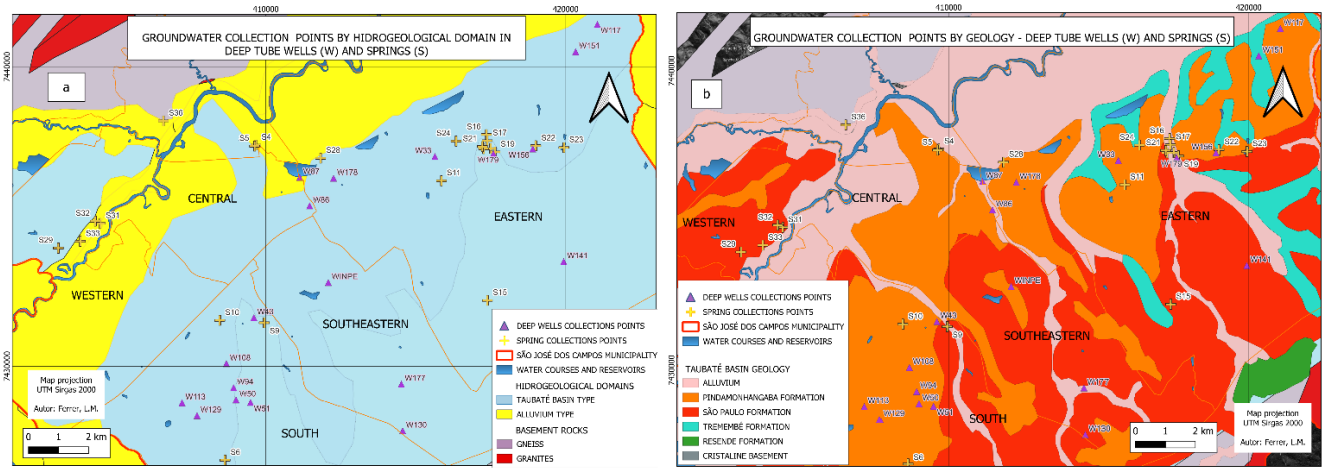

Figure 2. Hydrogeological domains and sampling locations in the study area. **(a)** Distribution of groundwater sampling points in deep tubular wells (purple triangles) and springs (yellow crosses) across the Alluvium and Taubaté Basin Types hydrogeological domains, covering the central, northern, southern, eastern, western, and southeastern sectors of São José dos Campos (SP). **(b)** Geological formations of the study area, showing the spatial relationship between sampling points and the underlying geological units.

By cross-referencing hydrogeological and geological maps (Dias et al., 2008; ANA, 2023) with the geographic coordinates of the sampling points, it was determined that 19 of the 20 deep tubular wells capture groundwater from the Taubaté Basin Type hydrogeological domain. The exception is well W87, which is located in the Alluvial Type domain (Fig. 2a). From a geological perspective, the wells are screened in units belonging to the Tremembé Formation (1 well), São Paulo Formation (2 wells), and Pindamonhangaba Formation (12 wells), as well as in Quaternary alluvial deposits (5 wells) (Table 1; Fig. 2b).

A similar spatial analysis was conducted for the springs. By overlaying hydrogeological and geological maps with the geographic coordinates of the sampling points, it was determined that 11 springs are located within the Taubaté Basin Type hydrogeological domain and 13 within the Alluvium Type hydrogeological domain (Fig. 2a). Geologically, 7 springs are associated with the São Paulo Formation, 9 with the Pindamonhangaba Formation, and 8 with Quaternary alluvial deposits (Table 2; Fig.2b).

2.2.1 Groundwater sampling and preservation

Two sampling campaigns were conducted in 2023: the first in February, representing the rainy season, and the second in July–August, corresponding to the dry season. A total of 84 groundwater samples were collected, comprising 44 samples during the rainy season (20 wells and 24 springs) and 40 samples during the dry season (19 wells and 21 springs).

All samples were collected within a maximum interval of one week during each campaign to ensure temporal comparability and minimize the influence of short-term meteorological variability on isotopic and physicochemical results.

During sampling, water was collected in 30 mL high-density polyethylene (HDPE) bottles. The bottles were filled completely and tightly sealed to avoid headspace formation and prevent potential isotopic exchange with atmospheric moisture.

After collection, the samples were stored in insulated containers protected from direct sunlight and transported to the laboratory on the same day. Upon arrival, they were refrigerated at 4 °C until isotopic analysis to preserve their physicochemical and isotopic integrity.

https://doi.org/10.5194/egusphere-2026-2557
Preprint. Discussion started: 15 June 2026

Table 1. Lithological and hydrogeological characterization of groundwater sampling points (deep wells) and associated isotope data.

Geological Formation	Hydrogeological Domain	ID Deep well	Wet season		Dry season	
			δ^{18} O	δ^{2} H	δ^{18} O	δ^{2} H
Pindamonhangaba	Taubaté Basin Type	W 043	-6.43	-38.72	-6.40	-43.47
		W 108	-7.25	-43.85	-	-
		W 094	-6.75	-40.49	-6.66	-44.58
		W 050	-6.43	-38.56	-6.41	-43.20
		W 051	-6.37	-36.93	-6.26	-40.59
		W 129	-6.43	-38.02	-6.29	-42.58
		W 113	-6.22	-37.16	-6.16	-41.13
		W 33	-6.74	-39.25	-6.65	-43.83
		W156	-7.18	-41.47	-7.00	-46.71
		W 117	-6.74	-38.03	-6.69	-42.98
		W 178	-7.03	-41.53	-6.88	-46.07
		W Inpe	-6.54	-38.26	-6.50	-43.12
São Paulo		W 130	-6.39	-35.61	-6.31	-40.39
		W 141	-7.71	-47.54	-7.22	-48.37
Tremembé		W 151	-7.55	-45.33	-7.19	-48.30
Alluvial deposits		W 114	-7.09	-41.14	-6.83	-44.79
		W 177	-6.96	-40.63	-6.80	-44.79
		W 179	-7.51	-44.91	-7.11	-46.99
		W 86	-6.80	-40.33	-6.76	-45.27
	Alluvium Type	W 87	-6.37	-37.46	-6.37	-42.94

2.3 Isotopic analyses and electrical conductivity

2.3.1 Isotopic analyses

Isotopic analyses were performed at the Isotopic Ecohydrology Laboratory (LabEcoh), part of the Division of Impacts, Adaptation, and Vulnerability of the National Institute for Space Research (DIIAV/INPE), located in São José dos Campos (SP), Brazil. Prior to analysis, all samples were filtered using 13 mm hydrophilized polytetrafluoroethylene (H-PTFE) syringe filters with a pore size of 0.22 µm to remove suspended particles and ensure analytical purity.

Table 2. Lithological and hydrogeological characterization of groundwater sampling points (springs) and associated isotope data.

Geological Formation	Hydrogeological Domain	ID Spring	Wet season		Dry season	
			δ^{18} O	δ^{2} H	δ^{18} O	δ^{2} H
	Taubaté Basin Type	S24	-6.44	-38.72	-5.27	-30.94
		S28	-6.5	-39.45	-2.62	-15.95
		S23	-6.62	-40.08	-5.63	-33.3
		S22	-6.52	-40.78	-5.32	-32.3

https://doi.org/10.5194/egusphere-2026-2557
Preprint. Discussion started: 15 June 2026

Pindamonhangaba		S10	-5.54	-31.55	-4.58	-25.83
		S07	-5.31	-31.49	-4.70	-27.96
		S06	-4.90	-26.71	-4.81	-27.88
	Alluvium Type	S05	-5.81	-32.55	-5.81	-34.63
		S04	-5.85	-33.03	-5.69	-34.82
São Paulo		S33	-5.35	-31.14	-5.23	-30.27
		S32	-5.38	-31.87	-5.35	-30.99
		S32b	-5.43	-30.47	-5.35	-30.99
		S31	-4.63	-25.76	-4.56	-25.77
		S31a	-5.15	-30.29	-	-
	Taubaté Basin Type	S29	-5.38	-30.84	-4.34	-25.41
		S15	-6.51	-36.39	-3.06	-16.98
Alluvial deposits		S21b	-5.86	-34.74	-5.7	-35.16
		S20	-7.61	-47.12	-	-
	Alluvium Type	S19	-6.53	-39.39	-5.54	-32.91
		S18	-6.48	-38.37	-6.15	-37.17
		S17	-6.13	-35.59	-6.08	-36.4
		S16	-5.97	-34.68	-4.58	-25.6
		S09	-5.29	-29.9	-4.87	-28.16
		S36	-5.13	-27.7	-4.66	-25.67

The isotopic composition of water, expressed as $\delta^{18}O$ and $\delta^{2}H$, was determined using cavity ring-down spectroscopy (CRDS) with a Picarro L2130-i isotopic water analyzer. Measurements were performed following the manufacturer's recommendations to minimize memory effects and instrumental drift.

The results were expressed relative to the Vienna Standard Mean Ocean Water (V-SMOW) international standard, as recommended by Coplen (1988). For calibration and normalization, internal secondary standards previously adjusted to the V-SMOW primary standard were used, in accordance with Eq. (1):

$$\delta‰ = \left(\frac{Rs}{R_{V-SMOW}} - 1\right) * 1000 \quad (1)$$

where R represents the ratio $^{18}O/^{16}O$ or $^{2}H/^{1}H$ in the sample (s) and in the reference standard (VSMOW).

Analytical precision was ±0.1‰ for $\delta^{18}O$ and ±0.5‰ for $\delta^{2}H$, as determined from repeated measurements of internal laboratory control standards throughout the analytical sequence.

Deuterium excess (d-excess) was calculated following Dansgaard (1964), in accordance Eq. (2):

$$d = \delta^{2}H - 8\delta^{18}O \quad (2)$$

The d-excess parameter provides complementary information on evaporation conditions at the moisture source and supports the interpretation of groundwater mixing and recharge processes.

2.3.2 Electrical conductivity (EC)

https://doi.org/10.5194/egusphere-2026-2557
Preprint. Discussion started: 15 June 2026

The electrical conductivity (EC) of groundwater samples collected from springs during the dry season was measured at the Isotopic Ecohydrology Laboratory (LabEcoh/INPE) using a Metrohm pH/conductivity meter (model 914), calibrated prior to analysis according to the manufacturer's specifications.

Electrical conductivity reflects the ability of water to conduct an electrical current as a function of its dissolved ionic content and is commonly used as a proxy for total dissolved solids. It provides insight into water–rock interactions and may also serve as an indirect indicator of anthropogenic influence or contamination.

In natural spring waters of the Taubaté Sedimentary Basin, EC values typically range between 10 and 100 µS cm^{-1} (Sundfeld et al., 2021). Values exceeding this range were interpreted as potential indicators of anthropogenic influence. In contrast, deeper groundwater abstracted from tubular wells generally exhibits higher EC values (180–350 µS cm^{-1}), reflecting longer flow paths, increased water–rock interaction, and greater residence times, which favor mineral dissolution (L'Apiccirella et al., 2017; Tirumalesh et al., 2017).

In this study, EC was used as an indicator of dissolved ion content to evaluate potential contamination in discharge areas and to assess differences between recharge zones associated with the investigated hydrogeological formations. The EC analysis also supported the interpretation of whether groundwater physicochemical characteristics reflect local anthropogenic pressures, particularly in areas experiencing significant land-use and land-cover changes due to urban expansion.

2.4 Precipitation data

The characterization of local precipitation during the study period (October 2022 to September 2023) was based on meteorological records obtained from a station operated by the National Center for Monitoring and Early Warning of Natural Disasters (CEMADEN), located in São José dos Campos (SP), Brazil (23°09′29.3″ S; 45°47′36.4″ W). These data were used to characterize prevailing meteorological conditions—including rainfall, air temperature, and relative humidity—during the rainy (February 2023) and dry (July–August 2023) sampling campaigns.

Event-based precipitation isotopic data (δ^2H and $\delta^{18}O$), corresponding to the same period as the groundwater sampling, were obtained from the database of the Isotopic Ecohydrology Laboratory (LabEcoh/INPE), as reported by Borma et al. (in submission). A total of 102 rainfall events were analyzed. All precipitation samples were processed and normalized following the same analytical protocol described in Section 2.3.1.

The isotopic composition of precipitation was used to construct the Local Meteoric Water Line (LMWL) for São José dos Campos. The LMWL served as a reference framework for interpreting groundwater isotopic signatures (wells and springs) and for inferring recharge sources, mixing processes, and potential evaporative effects within the local hydrogeological system.

2.5 Data processing and statistical analysis

The dataset was organized according to water source (deep wells or springs) and seasonal period (rainy and dry seasons). Statistical analyses were conducted to identify significant differences and to evaluate potential associations between isotopic and physicochemical parameters.

Differences in isotopic composition between groundwater sources (wells and springs) and between seasonal periods were assessed using analysis of variance (ANOVA), followed by Tukey's honestly significant difference (HSD) test for multiple

https://doi.org/10.5194/egusphere-2026-2557
Preprint. Discussion started: 15 June 2026

comparisons when appropriate.

Rainfall isotope data ($\delta^{18}O$, $\delta^{2}H$, and d-excess) were analyzed in relation to recorded precipitation (P, mm) in São José dos Campos to evaluate the influence of rainfall amount on isotopic composition.

Prior to correlation analyses between isotopic parameters and precipitation, data normality was assessed using the Shapiro–Wilk test. When deviations from normality were detected, Spearman's rank correlation coefficient was applied as a non-parametric measure of association. For normally distributed data, Pearson's correlation coefficient was used.

A significance level of $\alpha = 0.05$ was adopted for all statistical tests. All statistical analyses were performed using R software.

3 Results

3.1 Isotopic composition and seasonal variability

The $\delta^{18}O$ and $\delta^{2}H$ values of groundwater exhibited spatial and seasonal patterns (Fig. 3; Table 3).

Deep wells showed the most stable isotopic signatures. During the rainy season, mean $\delta^{18}O$ and $\delta^{2}H$ values were –6.75 ± 0.43‰ and –39.79 ± 3.06‰, respectively, while in the dry season they were –6.66 ± 0.32‰ and –44.22 ± 2.34‰. Seasonal differences were modest, and variability remained low.

Spring waters exhibited greater variability than deep wells. Mean $\delta^{18}O$ and $\delta^{2}H$ values were –5.85 ± 0.68‰ and –34.11 ± 5.02‰, respectively, in the rainy season, and –4.98 ± 0.84‰ and –29.21 ± 5.44‰ in the dry season.

Precipitation showed the highest isotopic variability among all sources. Mean $\delta^{18}O$ and $\delta^{2}H$ values were –4.86 ± 3.86‰ and –25.67 ± 31.72‰, respectively, in the rainy season, and –2.55 ± 3.46‰ and –5.57 ± 27.57‰ in the dry season (Fig.3; Table 3).

Seasonal enrichment during the dry period relative to the rainy season was generally observed, although its magnitude varied among water sources (Table 4). For $\delta^{18}O$, no significant seasonal difference was detected in deep well water ($p > 0.05$), whereas springs and precipitation showed significant differences between seasons ($p < 0.05$). For $\delta^{2}H$, significant seasonal differences were observed in all water groups ($p < 0.05$).

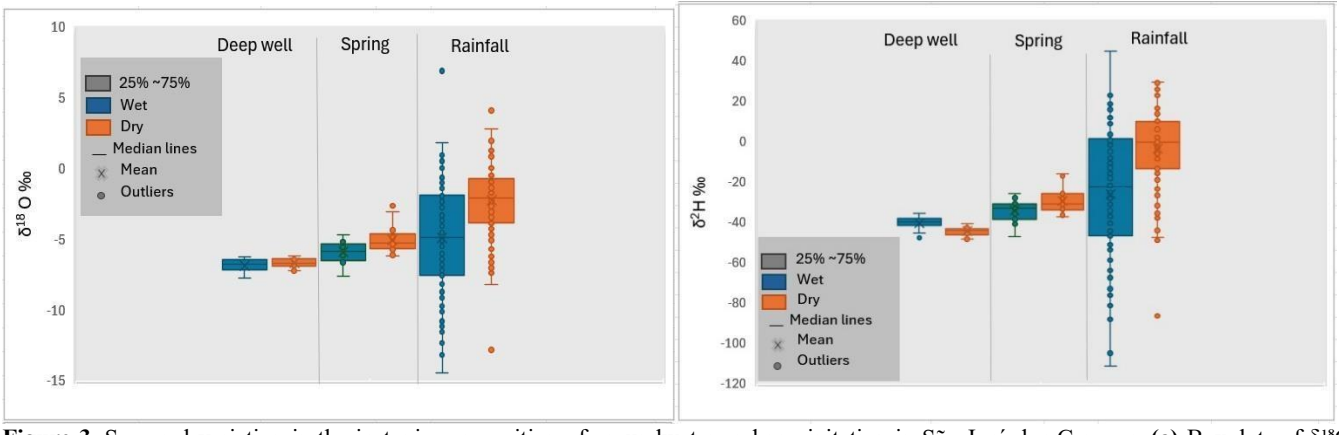

Figure 3. Seasonal variation in the isotopic composition of groundwater and precipitation in São José dos Campos. **(a)** Boxplots of $\delta^{18}O$ values and **(b)** $\delta^{2}H$ values for deep wells, springs, and precipitation during the rainy (wet) and dry seasons. Boxes represent the interquartile range (25th–75th percentiles), horizontal lines indicate medians, crosses denote mean values, whiskers represent the data range, and circles indicate outliers.

https://doi.org/10.5194/egusphere-2026-2557
Preprint. Discussion started: 15 June 2026

Table 3. Mean (± standard deviation) of δ^2H and $\delta^{18}O$ values for groundwater and precipitation in São José dos Campos (SJC), and the upper basin recharge area (São Francisco Xavier, SFX), during the rainy and dry seasons.

Mean and Standard deviation						
	Wet season (February 2023)			Dry season (July-August 2023)		
Sample	δ^{18} O	δ^2 H	d- excess	δ^{18} O	δ^2 H	d- excess
Deep wells	-6.75±0.43	-39.79±3.06	14.33±1.03	-6.66±0.32	-44.22± 2.34	9.04±0.81
Springs	-5.85±0.68	-34.11±5.02	12.66±1.11	-4.98±0.84	-29.21±5.44	10.64±1.65
SJC	-4.86±3.86	-25.67±31.72	13.18±5.35	-2.55±3.46	-5.57±27.57	14.85±4.88
SFX	-5.48±3.72	-27.50±31.06	11.55±5.58	-3.09±2.16	-8.49±18.71	16.27±6.36

Table 4. Statistical comparison of mean $\delta^{18}O$ and δ^2H values for groundwater (deep wells and springs) and precipitation in São José dos Campos during the wet and dry seasons. Identical letters indicate no significant difference between groups ($p > 0.05$), whereas different letters indicate significant differences among groups (Tukey HSD, $p < 0.05$).

All waters of the study area			
δ^{18} O			
season	**Deep wells**	**Springs**	**Rainfall**
wet	A	B	B
dry	A	A	A
δ^2 H			
season	**Deep wells**	**Springs**	**Rainfall**
wet	A	B	B
dry	B	A	A

Spring waters showed isotopic similarity to precipitation, with no significant differences ($p > 0.05$) for both $\delta^{18}O$ and δ^2H in either season, indicating a strong influence of recent recharge. In contrast, deep wells exhibited more complex behavior: for $\delta^{18}O$, similarity with precipitation was observed during the dry season, whereas significant differences occurred in the rainy season; for δ^2H, groundwater from deep wells differed significantly from precipitation in both seasons ($p < 0.05$).

3.2 Isotopic relationships in the dual isotopic space (δ^2H vs $\delta^{18}O$)

The isotopic composition of groundwater from deep wells and springs, plotted in dual-isotope space (δ^2H vs. $\delta^{18}O$), is presented in Fig. 4 a–c. The Local Meteorological Water Line (LMWL) for São José dos Campos plots slightly above the Global Meteoric Water Line (GMWL), with slopes close to the global value (~8), indicating predominantly meteoric origin of precipitation.

https://doi.org/10.5194/egusphere-2026-2557
Preprint. Discussion started: 15 June 2026

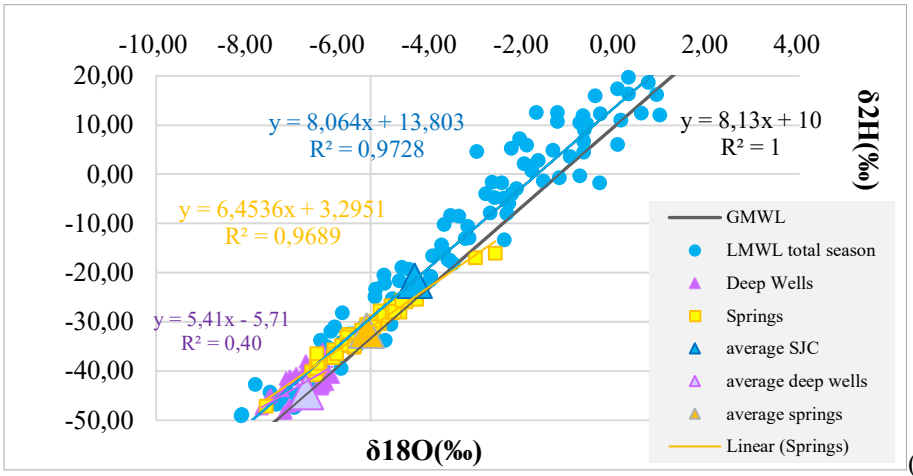

(a)

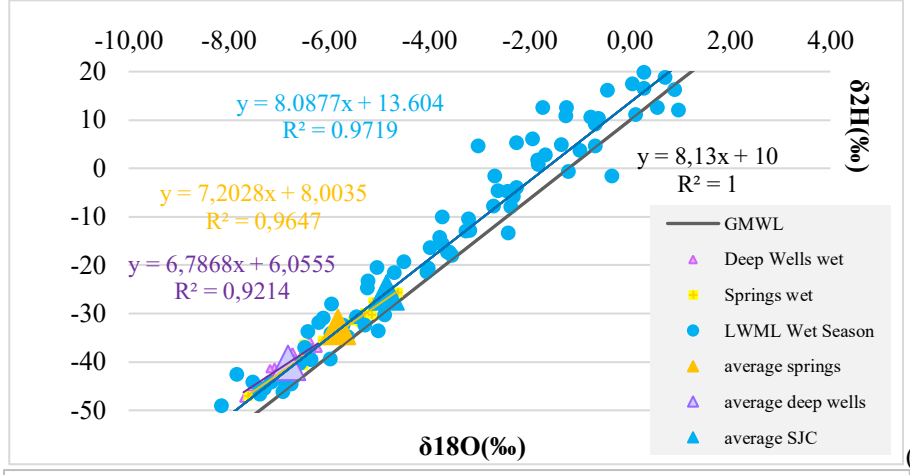

(b)

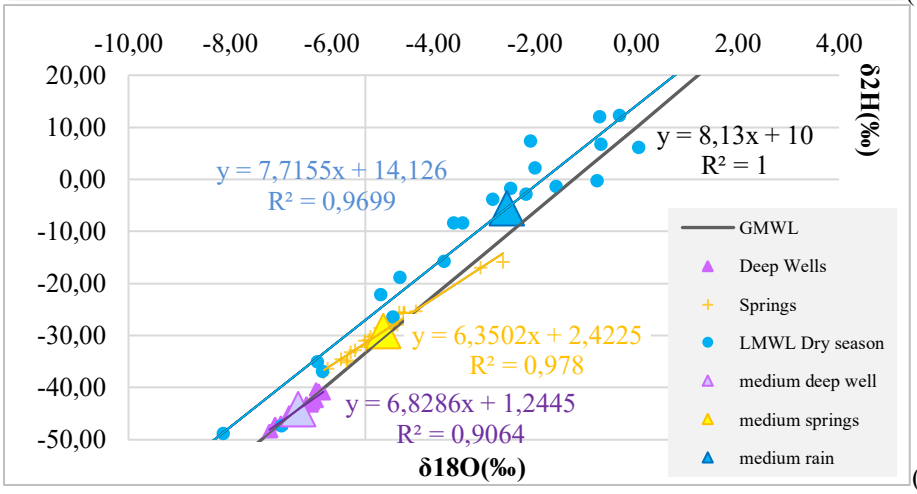

(c)

Figure 4. Isotopic relationships between groundwater and precipitation in dual-isotope space (δ^2H vs $\delta^{18}O$). **(a)** Combined dataset including groundwater samples (deep wells and springs) and the Local Meteoric Water Line (LMWL) derived from precipitation in the study area (São José dos Campos – SJC) for the full climatic period. **(b)** Rainy season (October 2022 to March 2023). **(c)** Dry season (April to September 2023).

https://doi.org/10.5194/egusphere-2026-2557
Preprint. Discussion started: 15 June 2026

During the rainy season (Fig. 4b), precipitation defined the LMWL according to the equation $y = 8.0877x + 13.604$ ($R^2 = 0.9719$), with a slope similar to that of the GMWL (8.13). Spring and deep well samples plotted close to the LMWL, showing strong linear correlations ($R^2 = 0.9647$ and 0.9214, respectively). However, their regression slopes were slightly lower (7.20 for springs and 6.78 for wells), indicating minor deviations from the meteoric line.

In the dry season (Fig. 4c), the LMWL followed the equation $y = 7.7155x + 14.126$ ($R^2 = 0.9699$), maintaining a slope comparable to that of the rainy season, but with a slightly higher intercept. Both springs and deep wells exhibited lower regression slopes relative to the LMWL, with values of 6.35 ($R^2 = 0.978$) and 6.83 ($R^2 = 0.906$), respectively. A systematic seasonal shift toward more enriched isotopic compositions was observed compared to the rainy season.

Across both seasons, deep well waters consistently displayed more depleted isotopic compositions and lower dispersion than spring waters. Springs generally plotted between the LMWL and the groundwater cluster, whereas deep wells tended to plot below the LMWL, particularly in the dry season.

The lowest regression slope was observed for springs during the dry season (6.35), followed by deep well water during the rainy season (6.78) (Fig. 4b; Table 5). These values are lower than the slopes of the LMWL (8.09) and GMWL (8.13), suggesting the influence of partial evaporation and/or isotopic mixing in waters near the discharge zone.

Table 5. Linear regression equations (δ^2H vs $\delta^{18}O$) and coefficients of determination (R^2) for precipitation and groundwater across different periods.

Local	Entire period	wet season	dry season
SJC rainfall	$\delta^2 H = 8.06\ \delta^{18} O + 13.80$ ($R^2 = 0.9728$)	$\delta^2 H = 8.09\ \delta^{18} O + 13.60$ ($R^2 = 0.9719$)	$\delta^2 H = 7.71\delta^{18} O + 14.12$ ($R^2 = 0.9699$)
SFX rainfall	$\delta^2 H = 8.34\ \delta^{18} O + 14.40$ ($R^2 = 0.9611$)	$\delta^2 H = 8.20\ \delta^{18} O + 12.67$ ($R^2 = 0.9685$)	$\delta^2 H = 8.14\ \delta^{18} O + 16.73$ ($R^2 = 0.8867$)
Deep wells	$\delta^2 H = 5.40\ \delta^{18} O - 5.71$ ($R^2 = 0.3966$)	$\delta^2H = 6.78\ \delta^{18}O + 6.05$ ($R^2 = 0.9214$)	$\delta^2 H = 6.82\delta^{18} O + 1.24$ ($R^2 = 0.9064$)
Springs	$\delta^2 H = 6.45\ \delta^{18} O + 3.29$ ($R^2 = 0.9689$)	$\delta^2 H = 7.20\ \delta^{18} O + 8.00$ ($R^2 = 0.9647$)	$\delta^2 H = 6.35\ \delta^{18} O + 2.42$ ($R^2 = 0.978$)

Overall, the regression slopes for groundwater (springs and wells) were consistently lower than those of the LMWL and GMWL (8.09–8.13), with the lowest values observed for springs during the dry season. This pattern indicates slight deviations from meteoric equilibrium and suggests the influence of secondary processes affecting groundwater isotopic signatures.

The intersection with the LMWL was limited. Among deep wells, only well W50 intersected the LMWL during the rainy season. Construction records (SP Águas, 2025) indicate that this well is associated with lithologies of the Caçapava and Tremembé formations and is located in a zone of strong geological interdigitation with alluvial deposits and the São Paulo Formation, which may favor hydraulic connectivity with more recently recharged waters.

For springs, intersections with the LMWL during the rainy season were observed at S24 (Pindamonhangaba Formation), S32a (São Paulo Formation), and S16 and S36 (alluvium). Overall, however, direct alignment with the meteoric line was limited.

https://doi.org/10.5194/egusphere-2026-2557
Preprint. Discussion started: 15 June 2026

3.3 Variability between hydrogeological formations

To evaluate whether lithology influences groundwater isotopic composition Tukey´s HSD test was applied to the $\delta^{18}O$ and $\delta^{2}H$ values of groundwater from deep wells and springs grouped according to geological formations.

For deep wells, no significant differences were detected between the Pindamonhangaba and Alluvial formations for either isotope ($p > 0.05$) (Fig. 5a and 5b; Table 6). For $\delta^{18}O$, no significant seasonal variation was observed between wet and dry periods. In contrast, $\delta^{2}H$ exhibited significant seasonal differences, although no differentiation between geological formations was detected within each season.

For springs, $\delta^{18}O$ also showed no significant differences among the Pindamonhangaba, Alluvial, and São Paulo formations in either season ($p > 0.05$). In contrast, $\delta^{2}H$ displayed seasonal and formation-dependent differences: during the rainy season, the Pindamonhangaba Formation differed significantly from the Alluvial and São Paulo formations ($p < 0.05$), while these latter two did not differ from each other (Fig. 5c and 5d; Table 6).

During the dry season, no significant isotopic differences were observed among geological formations for either deep wells or springs for both isotopes, indicating more homogeneous behavior under reduced precipitation conditions.

Overall, isotopic variability was more strongly associated with groundwater type (shallow versus deep) and seasonal effects rather than lithological differences within the Taubaté Basin. Deuterium ($\delta^{2}H$) showed greater sensitivity to seasonal variability, whereas $\delta^{18}O$ remained comparatively stable across formations and periods.

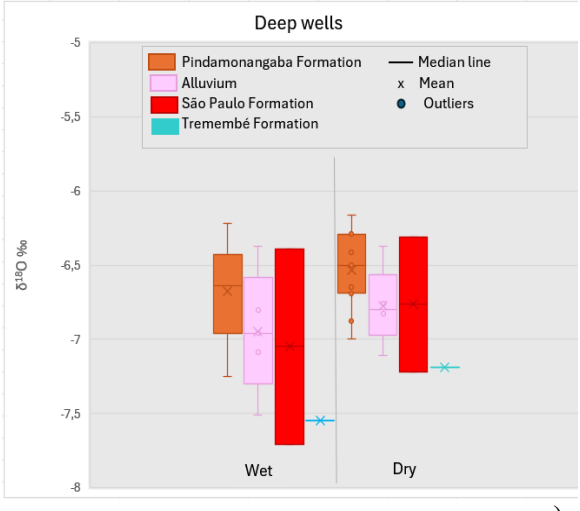

a)

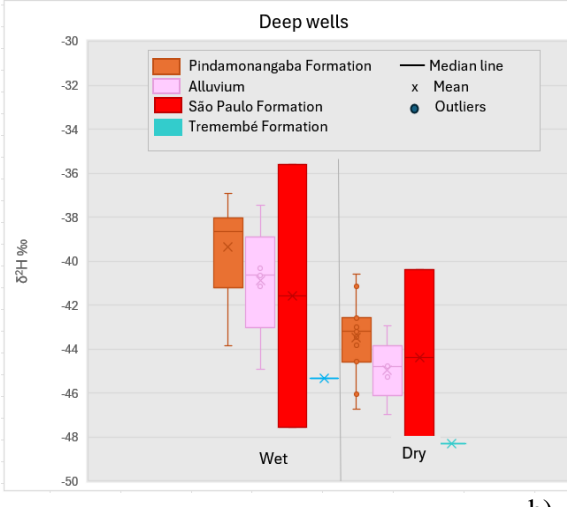

b)

https://doi.org/10.5194/egusphere-2026-2557
Preprint. Discussion started: 15 June 2026

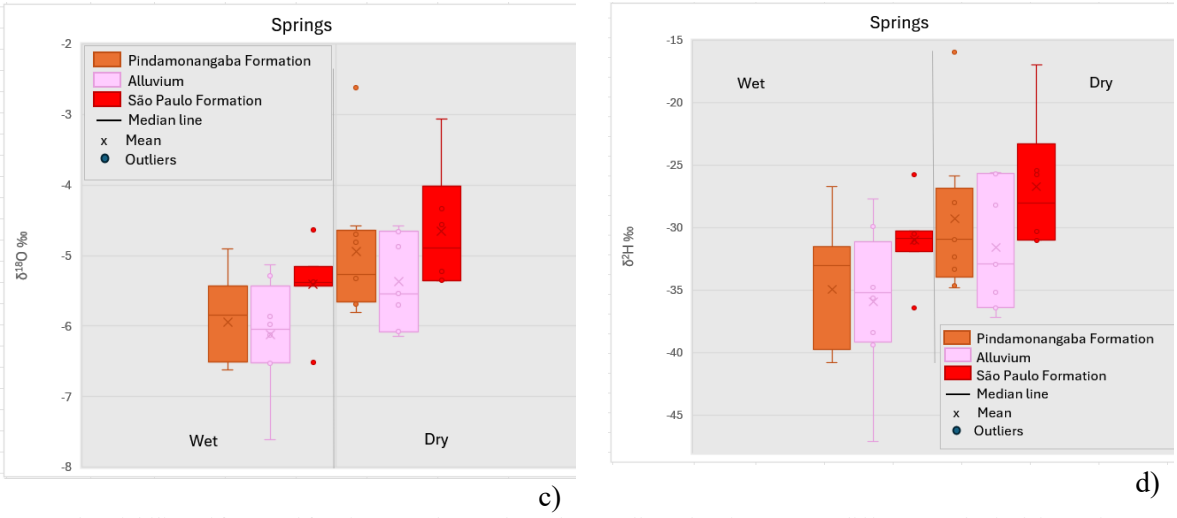

Figure 5. Seasonal variability of $\delta^{18}O$ and $\delta^{2}H$ in groundwater from deep wells and springs across different geological formations. **(a)** $\delta^{18}O$ in deep wells; **(b)** $\delta^{2}H$ in deep wells; **(c)** $\delta^{18}O$ in springs; **(d)** $\delta^{2}H$ in springs. Boxplots represent the distribution of isotopic values for the wet and dry seasons, grouped by geological formation (Pindamonhangaba, Alluvium, São Paulo, and Tremembé). The horizontal line within each box indicates the median, the "×" symbol represents the mean, and whiskers denote the range of the data. Outliers are shown as individual points.

Table 6. Tukey's HSD test results for $\delta^{18}O$ and $\delta^{2}H$ in groundwater from deep wells and springs grouped by geological formation and season. Different uppercase letters indicate statistically significant differences between groups ($p < 0.05$) within each row.

Deep well			Springs			
δ ^{18}O						
season	**Pindamonhangaba**	**Alluvium**	season	**Pindamonhangaba**	**Alluvium**	**São Paulo**
wet	A	A	wet	B	B	B
dry	A	A	dry	A	A	A
δ ^{2}H						
season	**Pindamonhangaba**	**Alluvium**	season	**Pindamonhangaba**	**Alluvium**	**São Paulo**
wet	A	A	wet	B	A	A
dry	B	B	dry	A	A	A

3.4 Electrical conductivity and relationship with d-excess

The d-excess values of spring waters were analyzed in relation to electrical conductivity (EC) (Fig. 6). Most samples showed relatively stable d-excess values within the range of 10–12%, indicating limited variability in moisture source conditions. However, samples S7, S10, and S15 deviated from this range.

Electrical conductivity values ranged from approximately 25 to over 600 µS/cm, indicating substantial variability among samples. While most springs exhibited relatively lower EC values (typically between 60–120 µS/cm) a subset of samples showed markedly elevated values.

No clear linear relationship between EC and d-excess was observed. However, samples with higher EC values tended to display greater dispersion in d-excess, including both values within the meteoric range and lower values, particularly during the dry season.

https://doi.org/10.5194/egusphere-2026-2557
Preprint. Discussion started: 15 June 2026

An additional sample (S28) exhibited both low EC and reduced d-excess (~5‰), deviating from the main cluster and indicating distinct isotopic behavior.

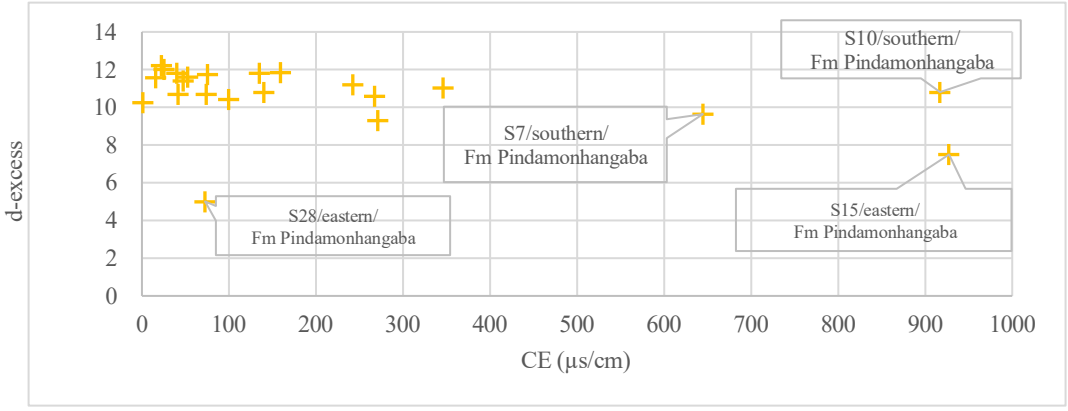

Figure 6. Relationship between d-excess and electrical conductivity (EC) in spring waters.

4 Discussion

4.1 Decoupling between local precipitation and deep groundwater recharge

The combined isotopic, statistical, and hydrogeological evidence indicates that groundwater recharge in the Taubaté Sedimentary Basin is predominantly indirect and regionally controlled, rather than locally driven by direct vertical infiltration. Although recharge occurs mainly during the rainy season—as expected for tropical climates (Jasechko et al., 2014; Bedaso & Wu, 2020)—intersections between groundwater and the LMWL were limited. Only one deep well (W50) and a limited number of springs (S16, S24, S32a, and S36) aligned directly with the local meteoric line (Figure4b). Most groundwater samples plotted below the LMWL and exhibited regression slopes lower than that of precipitation (Fig. 4a, 4b and 4c).

This systematic deviation suggests that groundwater isotopic composition is not a direct reflection of local rainfall but instead reflects the influence of delayed percolation, mixing processes, and potentially recharge occurring beyond the immediate sampling area. The reduced regression slopes observed for springs (6.45) and wells (5.41), compared to the LMWL (~8.06) (Fig. 4/ Table 5), further support the role of secondary processes affecting recharge prior to aquifer storage, consistent with non-conservative infiltration pathways (Gat, 1996).

The isotopic similarity between spring water and local precipitation suggests a stronger contribution from recent recharge. In contrast, the differences observed between deep well water and precipitation indicate indirect recharge, likely mediated by slower percolation and/or mixing within subsurface flow paths (Fig. 4/ Table 5). The absence of seasonal variability in $\delta^{18}O$ in deep well water (Fig.4/ Table 5) reinforces the interpretation of longer residence times in the sedimentary aquifers of the Taubaté Basin and reduced sensitivity to short-term climatic variability.

Overall, rather than representing a system dominated by rapid vertical infiltration, the isotopic evidence supports a basin-scale recharge mechanism in which groundwater integrates signals over space and time.

4.2 Regional recharge and altitude control

https://doi.org/10.5194/egusphere-2026-2557
Preprint. Discussion started: 15 June 2026

A key finding of this study is the closer isotopic correspondence between deep groundwater and precipitation from the upper basin (SFX) than with local rainfall in São José dos Campos. This pattern suggests that effective recharge may preferentially occur in higher-elevation zones and subsequently contribute to groundwater flow toward the lower, urbanized sector.

The altitude effect (Gonfiantini et al., 2001) and the tropical amount effect (Dansgaard, 1964) provide a mechanistic explanation for this pattern. Precipitation at higher elevations, typically more depleted in heavy isotopes and occasionally associated with higher d-excess values, shows greater similarity to groundwater signatures than locally measured rainfall.

This finding challenges the assumption that recharge in urban sedimentary basins is predominantly local. Instead, it supports a conceptual model in which recharge is spatially decoupled from discharge areas and controlled by regional physiographic gradients, particularly elevation.

4.3 Lithology versus flow depth: what controls isotopic signatures?

Despite the geological heterogeneity of the Taubaté Basin, statistical analysis revealed no significant isotopic differences between geological formations within either deep wells or springs. Instead, the most pronounced differentiation occurred between shallow (spring) and deep (wells) groundwater.

This pattern indicates that flow depth and residence time exert stronger control over isotopic composition than lithological variability. While the geological framework influences permeability and storage properties, isotopic signatures appear to be governed primarily by groundwater circulation dynamics and mixing processes.

The unique case of well W50—located within the upper stratigraphic Pindamonhangaba Formation and following alignment with the LMWL—illustrates that direct recharge may occur where stratigraphy and geomorphological conditions favor rapid infiltration. However, such conditions appear to be localized, and direct recharge pathways are not representative of the dominant recharge mechanism in the basin.

4.4 Processes controlling shallow groundwater variability

Electrical conductivity and d-excess analyses further differentiate shallow and deep systems. Most springs exhibited d-excess values near the canonical meteoric value (~10–12‰), indicating limited isotopic modification after recharge. However, a subset of springs located in more urbanized sectors (e.g., S7, S10, S15) showed elevated EC and modified isotopic signatures (Fig. 6).

Springs generally exhibited lower EC values (60–120 µS/cm) and greater variability, whereas deep wells showed higher and more stable EC values (180–350 µS/cm) (L'Apiccirella et al., 2017), consistent with longer flow paths and greater hydrochemical buffering at depth.

Samples with higher EC values tended to deviate from the main isotopic cluster, particularly during the dry season. In some cases, this was accompanied by lower d-excess values, suggesting the influence of evaporative processes prior to infiltration or during near-surface flow.

The occurrence of a sample with low electrical conductivity and reduced d-excess further indicates isotopic modification not associated with increased water–rock interaction. This pattern may reflect evaporation prior to infiltration or rapid recharge following partial evaporation, highlighting the influence of near-surface processes.

https://doi.org/10.5194/egusphere-2026-2557
Preprint. Discussion started: 15 June 2026

Overall, these patterns indicate that shallow groundwater is more sensitive to surface-related processes, including evaporation, short flow paths, and localized solute accumulation. In addition, urbanization and soil sealing may reduce direct vertical infiltration and promote lateral redistribution of water, reinforcing indirect recharge pathways and increasing the influence of near-surface processes on spring water composition.

4.5 A conceptual recharge model for the Taubaté Basin

The integrated isotopic, statistical, and hydrochemical evidence supports the existence of a dual groundwater recharge system in the Taubaté Sedimentary Basin.

A shallow system is expressed by springs that respond more directly to seasonal precipitation and reflect relatively rapid and spatially localized flow paths. In contrast, the deep system, represented by tubular wells, is characterized by predominantly indirect recharge, integration of regional groundwater flow, and longer residence times.

Although recharge intensifies during the rainy season, most deep groundwater does not originate from direct vertical infiltration at the point of abstraction. Instead, the isotopic similarity between deep groundwater and precipitation from higher-altitude recharge zones indicates that recharge is spatially displaced and regionally controlled. As a result, groundwater integrates isotopic signals over broader spatial scales before reaching the lower, urbanized sector of São José dos Campos.

This basin-scale integration provides a consistent explanation for several key observations:

(i) the reduced isotopic variability of deep groundwater relative to precipitation;

(ii) the weak seasonal signal in $\delta^{18}O$ in deep wells;

(iii) the limited alignment of groundwater samples with the LMWL; and

(iv) the absence of significant isotopic differentiation among geological formations.

Overall, the conceptual model highlights a clear decoupling between local precipitation and deep groundwater recharge, emphasizing the coexistence of rapid, shallow flow systems and slower, regionally integrated groundwater circulation within the sedimentary aquifer framework.

5 Conclusion

This study provides new insights into groundwater recharge processes in the Taubaté Sedimentary Basin based on integrated isotopic, statistical, and hydrochemical analyses. The main conclusions are:

(i) Groundwater recharge is predominantly indirect and spatially decoupled from local precipitation, with limited alignment between groundwater samples and the Local Meteoric Water Line (LMWL).

(ii) Deep groundwater exhibits reduced isotopic variability and weak seasonal signals, indicating longer residence times and integration of recharge processes over broader spatial and temporal scales.

(iii) A stronger isotopic correspondence between deep groundwater and precipitation from higher-altitude areas suggests that effective recharge occurs preferentially in elevated zones and contributes to regional groundwater flow toward lower urbanized sectors.

(iv) Isotopic composition is controlled primarily by flow depth and residence time rather than lithological variability within the basin.

https://doi.org/10.5194/egusphere-2026-2557
Preprint. Discussion started: 15 June 2026

(v) Shallow groundwater systems (springs) show greater variability and sensitivity to near-surface processes, including evaporation and short flow paths, as indicated by the relationship between electrical conductivity and d-excess.

(vi) The combined evidence supports a conceptual model of a dual groundwater system, characterized by the coexistence of rapid, shallow flow paths and slower, regionally integrated deep groundwater circulation.

Overall, these findings highlight the importance of considering spatially distributed recharge processes and multi-scale groundwater dynamics when assessing water resources in sedimentary basins under increasing urban pressure.

Electrical conductivity and d-excess analyses indicate that, despite intense urbanization in spring discharge areas, isotopic and chemical signals remain largely preserved, except in isolated locations affected by land-use change.

Over the past three decades, groundwater extraction rates in the eastern, southern, and southeastern sectors of São José dos Campos have declined by approximately 50%, coinciding with sustained population growth and high urban concentration. This long-term reduction in well yields highlights the vulnerability of urban groundwater systems and underscores the need for sustainable water management strategies under increasing climate variability and demand pressure. These results have direct implications for groundwater management, emphasizing the need to protect recharge areas located outside urban centers.

Authors' contributions. Text review and editing, drafting of the original manuscript, methodology, research, data curation: FerrerLM. Text review and editing, resources, methodology: BormaLS. English language review and editing: SakaguchiFH. Research: FerrerLM, MeneghetthiCD, PupinB, SakaguchiFH, SousaRCA. Project management: BormaLS. Resources, Project management: BormaLS.

Conflicts of interest. The corresponding author declared that none of the authors have any conflicts of interest.

Acknowledgments. The authors would like to thank all the reviewers who participated in the review, the CNPQ, which funded the research, and especially the Isotopic Ecohydrology Laboratory of the Division of Impacts, Adaptation, and Vulnerabilities at the National Institute for Space Research (LabEcoh/DIAV/INPE) for their support. Paragraphs of the manuscript were submitted to the generative artificial intelligence tool DeepSeek (version R1) to refine the language style to match the journal's requirements.

Funding. The research was funded by the National Council for Scientific and Technological Development (CNPQ). Grant nos.: 383510/2022-8, 381849/2023-6, 301163/2025-1, 314206/2025-6, 315484/2025-0, 315875/2025-9, 316351/2025-3, 319160/2025-4).

REFERENCES

Adomako, D.; Maloszewski, P.; Stumpp, C.; Osae, S.; Akiti, T. T. Estimation of groundwater recharge from depth profiles of water isotopes (d2H, d18O) in the Densu River basin, Ghana. Hydrological Sciences Journal, v. 55, n. 8, p. 1405–1416, https://doi.org/10.1080/02626667.2010.527847, 2010.

ANA [dataset], https://www.gov.br/ana/pt-br, 2023.

Barbosa, N. da S.; Barbosa, N. da S.; Salles, L. de Q. Methods for evaluating stable isotopes (δ^2 H and δ^{18} O) in hydrology: a

https://doi.org/10.5194/egusphere-2026-2557
Preprint. Discussion started: 15 June 2026

review. Terrae Didatica, v. 14, n. 2, p. 157–172, June 15,
https://periodicos.sbu.unicamp.br/ojs/index.php/td/article/view/8649972, 2018.

Bedaso, Z.; Wu, S. Y. Linking precipitation and groundwater isotopes in Ethiopia - Implications from local meteoric water lines and isoscapes. Journal of Hydrology, v. 596, n. September 2020, https://doi.org/10.1016/j.jhydrol.2021.12607, 2021.

CEMADEN [dataset], http://www2.cemaden.gov.br/mapainterativo/, 2023.

Cherry, M.; Gilmore, T.; Mittelstet, A.; Gastmans, D.; Santos, V.; Gates, J. B. Recharge seasonality based on stable isotopes: Nongrowing season bias altered by irrigation in Nebraska. Hydrological Processes, v. 34, n. 7, p. 1575–1586, https://doi.org/10.1002/hyp.13683, 2020.

Clark, I. & Fritz, P. Environmental Isotopes in Hydrogeology. New York, CRC Press. 328p., 1997. CLIMATE DATA [dataset], https://pt.climate-data.org/, 2023.

Coplen, T. B. Normalization of oxygen and hydrogen isotope data. Chemical Geology: Isotope Geoscience section, v. 72, n.4, p. 293–297, https://doi.org/10.1016/0168-9622(88)90042-5, 1988.

Craig, H. Isotopic variations in meteoric waters. Science, v. 133, n. 3465, p. 1702–1703 https://www.science.org/doi/10.1126/science.133.3465.1702, 1961.

Dansgaard, W. Stable isotopes in precipitation. Tellus, v. 16, n. 4, p. 436-468, https://doi.org/10.1111/j.2153-3490.1964.tb00181.x, 1964.

DEEPSEEK.DeepSeek-R1(or DeepThink). Hangzhou: DeepSeek, Artificial Intelligence, https://chat.deepseek.com/, 2025.

Dias, N.W.; Anjos, C.E.; Diniz, H.N.; Targa, M.S.; Lameira, W.J.M.; Rabelo, T.; Catelani, C.S.; Cundari, T.C. Recharge Project. Final Report. Characterization of recharge areas with integrated analysis of TM – Landsat orbital data and hydrogeological data, middle Paraíba do Sul River valley region, State of São Paulo. São José dos Campos. 2008, 149p. http://www.ipabhi.org/projeto-recarga/projeto-recarga-relatorio-final.pdf, 2023.

Döll, P.; Müller Schmied, H.; Schuh, C.; Portmann, F. T.; Eicker, A. Global-scale assessment of groundwater depletion and related groundwater abstractions: Combining hydrological modeling with information from well observations and Grace satellites. Water Resources Research, v. 50, n. 7, p. 5698–5720, Jul, http://doi.wiley.com/10.1002/2014WR015595, 2014.

Epstein, S.; Mayeda, T. S. Variation of O18 content of waters from natural sources. Geochimica et Cosmochimica Acta. v. 4, n. 5, p. 213-224, https://doi.org/10.1016/0016-7037(53)90051-9, 1953.

Estévez, E.; Rodríguez-Castillo T.; González-Ferreras, A.M.; Cañedo-Argüelles, M.; Barquín, J. Drivers of spatio-temporal patterns of salinity in Spanish rivers: a nationwide assessment. Phil. Trans. R. Soc. B 374: 20180022. . p. 1–10, 2018. http://dx.doi.org/10.1098/rstb.2018.0022.

Friedman, I. Deuterium content of natural waters and other substances. Geochimica et Cosmochimica Acta, v. 4, n. 1–2, p.89–103, 1953. https://doi.org/10.1016/0016-7037(53)90066-0

Gama, F. de A.; Fisch, S. Phenology of Tree Species in Areas of Riparian Vegetation Recovery in the Alambari Stream–São José dos Campos/SP. Revista Biociências, v.9, n. 2, p. 17-25, http://periodicos.unitau.br/ojs-2.2/index.php/biociencias/article/view/113, 2003.

https://doi.org/10.5194/egusphere-2026-2557
Preprint. Discussion started: 15 June 2026

Gat, J. R. Oxygen and hydrogen isotopes in the hydrologic cycle. Annual Review of Earth and Planetary Sciences, v. 24, n. 1, p. 225–262, https://www.annualreviews.org/doi/10.1146/annurev.earth.24.1.225,1996.

Gonfiantini, R.; Roche, M. A.; Olivry, J. C.; Fontes, J. C.; Zuppi, G. M. The altitude effect on the isotopic composition of tropical rains. Chemical Geology, v. 181, n. 1–4, p. 147–167, https://doi.org/10.1016/S0009-2541(01)00279-0, 2001.

Gupta, P.; Noone, D.; Galewsky, J.; Sweeney, C.; Vaughn, B. H. Demonstration of high-precision continuous measurements of water vapor isotopologues in laboratory and remote field deployments using wavelength-scanned cavity ring-down spectroscopy (WS-CRDS) technology. Rapid Communications in Mass Spectrometry, v. 23, n. 16, p. 2534–2542, https://analyticalsciencejournals.onlinelibrary.wiley.com/doi/10.1002/rcm.4100, 2009.

IBGE [dataset], https://www.ibge.gov.br/, 2023.

INMET [dataset] https://clima.inmet.gov.br/prec, 2023.

IPCC: Summary for Policymakers [H.-O. Pörtner, D.C. Roberts, E.S. Poloczanska, K. Mintenbeck, M. Tignor, A. Alegría, M. Craig, S. Langsdorf, S. Löschke, V. Möller, A. Okem (eds.)]. In: Climate Change 2022: Impacts, Adaptation and Vulnerability. Contribution of Working Group II to the Sixth Assessment Report of the Intergovernmental Panel on Climate Change [H.-O. Pörtner, D.C. Roberts, M. Tignor, E.S. Poloczanska, K. Mintenbeck, A. Alegría, M. Craig, S. Langsdorf, S. Löschke, V. Möller, A. Okem, B. Rama (eds.)]. Cambridge University Press, Cambridge, UK and New York, NY, USA, pp.3–33, doi:10.1017/9781009325844.001, 2022.

Jasechko, S.; Birks, S. J.; Gleeson, T.; Wada, Y.; Fawcett, P. J.; sharp, Z. D.; Mcdonnell, J. J.; Welker, J. M. The pronounced seasonality of global groundwater recharge. Water Resources Research, v. 50, n. 11, p. 8845–8867, https://doi.org/10.1002/2014WR015809, 2014.

Jobbágy, E. G.; Jackson, R. B. Groundwater use, and salinization with grassland afforestation. Global Change Biology, v. 10, n. 8, p. 1299–1312, https://doi.org/10.1111/j.1365-2486.2004.00806.x, 2004.

L'apiccirella, E.; Delatim Simonato, M.; Leitão, A.; Ferreira Brandão, D.; Campos, J. E. Hydrogeochemistry of São José Dos Campos, Jacareí, and Caçapava, in the Paraíba Do Sul Valley. Groundwater, p. 1–20, https://doi.org/10.14295/ras.v0i0.28727, 2017.

Liberoff, A. L.; Poca, M. Science of the Total Environment Groundwater-surface water interactions in a semi-arid irrigated agricultural valley: A hydrometric and tracer-aided approach. Science of the Total Environment, v. 903, n. June, p. 166625, https://doi.org/10.1016/j.scitotenv.2023.166625, 2023.

Machida, I.; Ono, M.; Kamitani, T.; Muranaka, Y. Applicability of d-excess and 17O-excess as groundwater tracers for determination of recharge area. Hydrogeology Journal, v. 30, n. 7, p. 2027–2041, https://doi.org/10.1007/s10040-022-02526-0, 2022.

Mcguire, K., Mcdonnell, J., Stable isotope tracers in watershed hydrology. In: Michener, R.H., Lajtha, K. (Eds.), Stable Isotopes in Ecology and Environmental Science. Blackwell Publishing, 634 pp. 334-374, 2007.

Oliveira, A. S. de; Salati, E. A study on groundwater in the Piracicaba region. Annals of the Luiz de Queiroz School of Agriculture, v. 38, n. 2, p. 885–907, https://www.scielo.br/j/aesalq/a/xxZN4dr5ZGqLSRYk3PTKTtw/?lang=pt, 1981.

https://doi.org/10.5194/egusphere-2026-2557
Preprint. Discussion started: 15 June 2026

Re, V.; Thin, M. M.; Tringali, C.; Mya, M.; Destefanis, E.; Sacchi, E. Laying the groundwork for raising awareness on water-related issues with a socio-hydrogeological approach: The Inle Lake case study (southern Shan State, Myanmar). Water (Switzerland), v. 13, n. 17, https://doi.org/10.3390/w13172434, 2021.

Riccomini, C. The Continental Rift of Southeastern Brazil. Doctoral thesis, Institute of Geosciences, University of São Paulo, São Paulo, p. 319, 1989.

Rozanski, K.; Araguás-Araguás, L.; Gonfiantini, R., Isotopic Patterns in Modern Global Precipitation. *In*: Continental Isotopic Indicators of Climate, American Geophysical Union Monograph p. 1–36, 1993.

Sacchi, M. D.; Manzione, R. L.; Gastmans, D.; Donadelli, M.; Manzione, R. L.; Gastmans, D. How much rainwater contributes to a spring discharge in the Guarani Aquifer System: insights from stable isotopes and a mass balance model. Isotopes in Environmental and Health Studies ISSN: 2024. https://doi.org/10.1080/10256016.2024.2397469

SGB [dataset]. http://www.cprm.gov.br/, 2023.

SP ÁGUAS [dataset] https://www.spaguas.sp.gov.br/site/, 2025.

Stahl, M. O.; Gehring, J.; Jameel, Y. Isotopic variation in groundwater across the conterminous United States – Insight into hydrologic processes. Hydrological Processes, v. 34, n. 16, p. 3506–3523, https://doi.org/10.1002/hyp.13832, 2020.

Sundfeld, A.; Farinha, E.M.K.; Fiore, F.A.; Murakami, L.Y.K.; Machado, L.R.M.; Ribeiro, M.R. The springs and the city: a look at São José dos Campos.1 ed. São Paulo. Academic Culture. 228p., ISBN: 978-65-59540-51-8, 2021.

Tirumalesh, K.; Sharma, D. A.; Madhuri, S.; Pant, D.; Mohokar, H. V; Kumar, A.; Sinha, U. K. Isotope investigation on groundwater recharge and dynamics in shallow and deep alluvial aquifers of southwest Punjab. V. 129, p. 163-170, Applied Radiation and Isotopes. http://dx.doi.org/10.1016/j.apradiso.2017.07.022, 2017.

Vidal, A. C.; Fernandes, F. L.; Kiang, C. H. Distribution of sandstones in the Taubaté Basin – SP. Geociências, v. 23, n. 1/2, p. 55–66, ISSN 1980-900X (online), 2004.

Vörösmarty, C. J.; Green, P.; Salisbury, J.; Lammers, R. B. Global water resources: Vulnerability from climate change and population growth. Science, v. 289, n. 5477, p. 284–288, https://doi.org/10.1126/science.289.5477.284, 2000.

Yoshinaga, S.; de Silva, A. A. K.; Matsui, E. Stable isotopes use in hydrogeology studies of mineral and thermal waters (Lindoia region, Sao Paulo, Brazil). Stable isotopes use in hydrogeology studies of mineral and thermal waters (Lindoia region, São Paulo, Brazil) . International Nuclear Information System - INIS, v. 26, n. 9, https://inis.iaea.org/collection/NCLCollectionStore/_Public/26/032/26032770.pdf?r=1, 1991.

Yoshioka, Y.; Yoshioka, H. Spatiotemporal variability of hydrogen stable isotopes at a local scale in shallow groundwater during the warm season in Tottori Prefecture, Japan. Hydrological Research Letters, v. 16, n. 1, p. 25–31, https://doi.org/10.3178/hrl.16.25, 2022.

Appendix A

Deep tubular wells of the Paraíba Subsystem, rainwater and springs sampled in the municipality of São José dos Campos, SP. The depth, production flow (m³/h), and other hydrogeological parameters of the deep tubular wells were obtained from previous

https://doi.org/10.5194/egusphere-2026-2557
Preprint. Discussion started: 15 June 2026

records and publications (Vidal et al., 2004; L'Apiccirella et al., 2012; SGB, 2023; SP Águas, 2025) (Table A1, A2, and A3).

Table A1. Deep tubular wells of the Paraíba Subsystem sampled in the municipality of São José dos Campos, SP

ID Deep well	Wet season			Dry season			E (UTM)	N (UTM)	Neighborhood/ Region	Flow rate (m^3/h)	Depth of use (m)
	δ^{18} O	δ^2 H	d-excess	δ^{18} O	δ^2 H	d-excess					
W 043	-6.43	-38.72	12.72	-6.4	-43.47	7.73	409603.9757	7431622.7612	Jd Satélite/ South	479	100
W 108	-7.25	-43.85	14.15	-	-	-	408686.3409	7430086.5510	Jd Satélite/ South	527	150
W 094	-6.75	-40.49	13.51	-6.66	-44.58	8.7	408926.8685	7429283.4710	Eucalyptus Forest/South	1393	100
W 050	-6.43	-38.56	12.88	-6.41	-43.2	8.08	409007.8670	7428876.3455	alyptus Forest/ South	55	100
W 051	-6.37	-36.93	14.03	-6.26	-40.59	9.49	409491.2358	7428790.0066	Eucalyptus Forest/South	495	100
W 129	-6.43	-38.02	13.42	-6.29	-42.58	7.74	407708.3880	7428351.9894	d Morumbi/ South	30	100
W 113	-6.22	-37.16	12.6	-6.16	-41.13	8.15	407,206.5710	7428780.7816	d Morumbi/ South	35	100
W 33	-6.74	-39.25	14.67	-6.65	-43.83	9.37	415,640.8381	7437004.4459	. Motorama/ East	475	200
W156	-7.18	-41.47	15.97	-7	-46.71	9.29	418,904.6985	7437258.8439	Santa Inês III/ East	8735	232
W 117	-6.74	-38.03	15.89	-6.69	-42.98	10.54	421057.9463	7441416.6590	Cj. Res. Galo Branco/ East	4321	104.5
W 178	-7.03	-41.53	14.71	-6.88	-46.07	8.97	412260.8827	7436277.0667	la Tatetuba/ East	90	203
W Inpe	-6.54	-38.26	14.06	-6.5	-43.12	8.88	412085.8363	7432794.0191	ardim da Granja/ Southeast	15	170
W 130	-6.39	-35.61	15.51	-6.31	-40.39	10.09	414565.5367	7427841.1432	Jd São Judas Tadeu/ Southeast	50	100
W 141	-7.71	-47.54	14.14	-7.22	-48.37	9.39	419936.5694	7433495.0829	Nova Esperança/East Park	-	
W 151	-7.55	-45.33	15.07	-7.19	-48.3	9.22	420336.7232	7440503.5464	Jd. Itapuã/ East	7977	229.4
W 114	-7.09	-41.14	15.58	-6.83	-44.79	9.85	411667.0049	7426375.4848	Interlagos Park/Southeast	-	-
W 177	-6.96	-40.63	15.05	-6.8	-44.79	9.61	414522.4102	7429403.1524	Jd. Santa Luzia/ Southeast	-	-
W 179	-7.51	-44.91	15.17	-7.11	-46.99	9.89	417592.0705	7437095.9514	Pararangaba/ East	50	200
W 86	-6.8	-40.33	14.07	-6.76	-45.27	8.81	411463.1761	7435357.1273	a Corintinha/ East	139	100
W 87	-6.37	-37.46	13.5	-6.37	-42.94	8.02	411132.6600	7436307.9675	Vila Lúcia/ East	42	100

Table A2: Springs sampled in the study area

ID Spring	Wet season			Dry season			E (UTM)	N (UTM)	Neighborhood/Region
	δ^{18} O	δ^2 H	d-excess	δ^{18} O	δ^2 H	d-excess			
S24	-6.44	-38.72	12.8	-5.27	-30.94	11.22	416,347	7,437,518	São Vicente/East Garden
S28	-6.5	-39.45	12.55	-2.62	-15.95	5.01	411829	7436948	Vista Linda/East Residential
S23	-6.62	-40.08	12.88	-5.63	-33.3	11.74	419942	7437304	Jardim São José/East
S22	-6.52	-40.78	11.38	-5.32	-32.3	10.26	419005	7437365	Santa Inês III/East Garden
S10	-5.54	-31.55	12.77	-4.58	-25.83	10.81	408,465	7431533	Satellite Garden/South
S07	-5.31	-31.49	10.99	-4.7	-27.96	9.64	409,208	7426328	Campo dos Alemães/South
S06	-4.9	-26.71	12.49	-4.81	-27.88	10.6	408,640	7,426,864	Altos do Bosque/South
S05	-5.81	-32.55	13.93	-5.81	-34.63	11.85	409,627	7437351	Santana – City Park/North
S04	-5.85	-33.03	13.77	-5.69	-34.82	10.7	409,668	7,437,386	Santana – City Park/North
S33	-5.35	-31.14	11.66	-5.23	-30.27	11.57	403814	7434174	ldorado Condominium/ West

https://doi.org/10.5194/egusphere-2026-2557
Preprint. Discussion started: 15 June 2026

S32	-5.38	-31.87	11.17	-5.35	-30.99	11.81	404314	7434845	Urbanova – Portal da Serra Condominium/ West
S32a	-5.43	-30.47	12.97	-5.05	-28.59	11.81	404314	7434845	ova – Portal da Serra/Oeste Condominium
S31	-4.63	-25.76	11.28	-4.56	-25.77	10.71	404,478	7434769	ova – Cond. Morada da Serra/West
S31a	-5.15	-30.29	10.91	-	-	-	404,478	7434769	ova – Cond. Morada da Serra/West
S29	-5.38	-30.84	12.2	-4.34	-25.41	9.31	403081	7433946	ova – Altos da Serra/Oeste Condominium
S15	-6.51	-36.39	15.69	-3.06	-16.98	7.5	417,393	7,432,198	Mariana II/East Garden
S21	-5.86	-34.74	12.14	-5.7	-35.16	10.44	417,225	7,437,336	Parangaba/East Garden
S20	-7.61	-47.12	13.76	-	-	-	417,265	7437266	Parangaba/East Garden
S19	-6.53	-39.39	12.85	-5.54	-32.91	11.41	417,650	7,437,158	California/East Garden
S18	-6.48	-38.37	13.47	-6.15	-37.17	12.03	417,496	7,437,271	California/East Garden
S17	-6.13	-35.59	13.45	-6.08	-36.4	12.24	417,385	7437532	California/East Garden
S16	-5.97	-34.68	13.08	-4.58	-25.6	11.04	417,356	7437737	California/East Garden
S09	-5.29	-29.9	12.42	-4.87	-28.16	10.8	409948	7431453	Satellite Garden/South
S36	-5.13	-27.7	13.34	-4.66	-25.67	11.61	406,595	7,438,192	Santana Alberto Simões Park/North

Table A3: Values of $\delta^{18}O$ and $\delta^{2}H$ measured in rainwater from the study area and calculation of the d-excess of the (SJC).

Seasonal weather pattern	Sampling date	δ^{18} O	δ^{2} H	d excess= δ^{2} H – 8 * δ^{18} O
Wet	10/01/2022	-2.44	-4.87	14.65
	10/07/2022	-0.45	16.03	19.63
	10/10/2022	0.04	17.40	17.08
	10/10/2022	-0.69	9.09	14.61
	10/13/2022	6.90	45.02	-10.18
	10/18/2022	0.11	11.02	10.14
	10/19/2022	0.70	18.72	13.12
	10/21/2022	1.03	20.73	12.49
	10/21/2022	0.27	16.42	14.26
	10/21/2022	0.55	12.47	8.07
	10/29/2022	1.87	25.25	10.29
	10/31/2022	0.27	19.81	17.65
	10/31/2022	-5.95	-28.08	19.52
	10/31/2022	-6.21	-31.88	17.8
	11/01/2022	-3.75	-15.61	14.39
	11/03/2022	-1.28	10.79	21.03
	11/07/2022	-3.03	4.61	28.85
	11/07/2022	-1.74	12.55	26.47
	11/09/2022	-1.94	5.99	21.51
	11/10/2022	-2.27	5.26	23.42
	11/11/2022	-1.27	12.58	22.74
	11/16/2022	-0.79	10.55	16.87

https://doi.org/10.5194/egusphere-2026-2557
Preprint. Discussion started: 15 June 2026

	11/21/2022	1.10	23.02	14.22
	11/23/2022	-2.70	-1.60	20
	11/23/2022	-2.33	-5.88	12.76
	11/24/2022	-5.97	-34.15	13.61
	11/25/2022	-2.43	-13.34	6.1
	11/28/2022	-6.88	-44.64	10.4
	11/29/2022	-7.53	-44.23	16.01
	11/29/2022	-8.15	-49.06	16.14
	11/30/2022	-7.29	-45.56	12.76
	12/01/2022	-6.43	-33.73	17.71
	12/05/2022	-8.04	-50.88	13.44
	12/05/2022	-7.85	-53.12	9.68
	12/06/2022	-6.76	-44.59	9.49
	12/06/2022	-9.46	-63.67	12.01
	12/06/2022	-10.09	-67.43	13.29
	12/07/2022	-11.51	-76.05	16.03
	12/08/2022	-8.01	-58.61	5.47
	12/12/2022	-1.84	1.67	16.39
	12/13/2022	-5.29	-32.45	9.87
	12/13/2022	-12.16	-81.08	16.2
	12/13/2022	-11.14	-75.16	13.96
	12/19/2022	-1.83	0.73	15.37
	12/20/2022	-1.69	2.79	16.31
	12/20/2022	-3.99	-16.48	15.44
	12/21/2022	-6.37	-39.62	11.34
	12/21/2022	-6.82	-52.53	2.03
	12/22/2022	-0.36	-1.68	1.2
	12/26/2022	-8.48	-62.84	5
	01/02/2023	-12.30	-87.87	10.53
	01/04/2023	-5.98	-39.44	8.4
	01/05/2023	-9.70	-67.27	10.33
	01/06/2023	-8.53	-53.43	14.81
	01/09/2023	-3.65	-17.35	11.85
	01/09/2023	-6.93	-46.16	9.28
	01/10/2023	-5.02	-33.67	6.49
	11/01/2023	-13.16	-104.86	0.42
	01/12/2023	-14.44	-110.95	4.57
	01/13/2023	-10.67	-74.39	10.97
	01/16/2023	-9.87	-75.46	3.5

https://doi.org/10.5194/egusphere-2026-2557
Preprint. Discussion started: 15 June 2026

	01/18/2023	-4.89	-30.38	8.74
	01/19/2023	-2.38	-7.95	11.09
	01/19/2023	-4.05	-21.50	10.9
	01/20/2023	-4.03	-20.73	11.51
	01/20/2023	-5.63	-34.78	10.26
	01/23/2023	-6.59	-40.31	12.41
	01/24/2023	-4.71	-21.64	16.04
	01/30/2023	-11.30	-80.74	9.66
	01/30/2023	-10.64	-72.95	12.17
	01/30/2023	-9.13	-61.34	11.7
	01/31/2023	-10.96	-72.73	14.95
	02/01/2023	-8.69	-51.96	17.56
	02/02/2023	-5.72	-32.43	13.33
	02/03/2023	-5.80	-32.45	13.95
	02/06/2023	-3.22	-10.53	15.23
	02/06/2023	-6.69	-42.89	10.63
	02/06/2023	-7.84	-51.58	11.14
	02/07/2023	-10.77	-74.33	11.83
	02/07/2023	-9.80	-62.18	16.22
	02/08/2023	-7.15	-44.22	12.98
	02/08/2023	-7.85	-42.64	20.16
	02/10/2023	-4.51	-19.31	16.77
	02/10/2023	-1.23	-0.65	9.19
	02/13/2023	-5.05	-20.49	19.91
	02/15/2023	-7.39	-46.75	12.37
	02/16/2023	-1.00	3.66	11.66
	02/17/2023	-5.23	-23.28	18.56
	02/22/2023	-3.20	-12.87	12.73
	02/24/2023	-5.24	-24.80	17.12
	02/24/2023	-3.80	-15.49	14.91
	02/27/2023	-3.55	-18.03	10.37
	02/28/2023	-6.12	-30.95	18.01
	03/01/2023	-6.49	-37.04	14.88
	03/02/2023	-3.80	-14.35	16.05
	03/03/2023	-0.70	4.53	10.13
	03/06/2023	-3.28	-13.00	13.24
	03/06/2023	0.96	12.05	4.37
	03/09/2023	0.89	16.28	9.16
	03/10/2023	-2.73	-7.86	13.98

https://doi.org/10.5194/egusphere-2026-2557
Preprint. Discussion started: 15 June 2026

	03/13/2023	-3.74	-10.11	19.81
	03/13/2023	-5.46	-30.69	12.99
	03/14/2023	-4.86	-25.20	13.68
	03/14/2023	-3.61	-17.41	11.47
	03/15/2023	-2.26	-3.97	14.11
	03/21/2023	-1.37	4.88	15.84
	03/27/2023	-0.63	10.24	15.28
	30/03/2023	-2.64	-4.71	16.41
Dry	04/03/2023	-1.58	-1.33	11.31
	04/10/2023	-2.83	-3.86	18.78
	04/14/2023	-8.14	-48.78	16.34
	04/18/2023	-6.99	-47.36	8.56
	04/19/2023	-12.80	-86.25	16.15
	04/27/2023	-0.70	6.79	12.39
	04/28/2023	-5.04	-22.07	18.25
	05/02/2023	-2.17	-2.81	14.55
	05/29/2023	-0.78	-0.22	6.02
	05/31/2023	-3.60	-8.34	20.46
	05/31/2023	-4.66	-18.83	18.45
	06/14/2023	-3.42	-8.40	18.96
	06/15/2023	-4.80	-26.44	11.96
	06/15/2023	-3.79	-15.68	14.64
	06/15/2023	-6.29	-35.01	15.31
	06/16/2023	-6.18	-36.92	12.52
	07/10/2023	1.96	29.26	13.58
	07/31/2023	0.04	6.16	5.84
	08/25/2023	2.28	25.99	7.75
	08/28/2023	-2.09	7.32	24.04
	09/04/2023	-0.72	11.99	17.75
	09/05/2023	2.83	27.75	5.11
	09/14/2023	-0.34	12.30	15.02
	09/15/2023	-2.48	-1.76	18.08
	09/27/2023	0.96	23.03	15.35
	09/27/2023	0.96	26.96	19.28
	09/28/2023	0.88	28.27	21.23
	09/28/2023	-2.00	2.19	18.19

545